

# SPHERE: The VLT exo-planet imager in the post-FDR phase

Francois Wildi<sup>1</sup>, Jean-Luc Beuzit<sup>b</sup>, Markus Feldt<sup>c</sup>, David Mouillet<sup>b</sup>, Kjetil Dohlen<sup>a</sup>, Pascal Puget<sup>b</sup>, Andrea Baruffolo<sup>d</sup>, Julien Charton<sup>b</sup>, Pierre Baudoz<sup>c</sup>, Anthony Boccaletti<sup>e</sup>, Lyu Abe<sup>f</sup>, Riccardo Claudi<sup>d</sup>, Philippe Feautrier<sup>b</sup>, Thierry Fusco<sup>g</sup>, Raffaele Gratton<sup>d</sup>, Norbert Hubin<sup>h</sup>, Markus Kasper<sup>h</sup>, Maud Langlois<sup>a</sup>, Rainer Lenzen<sup>c</sup>, Alexey Pavlov<sup>c</sup>, Cyril Petit<sup>g</sup>, Johan Pragt<sup>i</sup>, Patrick Rabou<sup>b</sup>, Ronald Roelfsema<sup>l</sup>, Michel Saisse<sup>a</sup>, Hans-Martin Schmid<sup>l</sup>, Eric Stadler<sup>b</sup>, Claire Moutou<sup>a</sup>, Massimo Turatto<sup>d</sup>, Stéphane Udry<sup>l</sup>, Rens Waters<sup>k</sup>, Thomas Henning<sup>c</sup>, Anne-Marie Lagrange<sup>l</sup>, Farrokh Vakili<sup>f</sup>.

<sup>1</sup> Observatoire de Genève, CH-1290 Sauverny, Switzerland

<sup>a</sup> Laboratoire d'Astrophysique de Marseille, B.P. 8, F-13376 Marseille Cedex 12, France

<sup>b</sup> Laboratoire d'Astrophysique de Grenoble, B.P. 53, F-38041 Grenoble Cedex 9, France

<sup>c</sup> Max Planck Institut für Astronomie, Königstuhl 17, D-69117 Heidelberg, Germany

<sup>d</sup> Osservatorio Astronomico di Padova, Vicolo dell'Osservatorio 5, I-35122 Padova, Italy

<sup>e</sup> Laboratoire d'Etudes Spatiales et d'Instrumentation en Astrophysique, F-92190 Meudon, France

<sup>f</sup> Laboratoire Universitaire d'Astrophysique de Nice, Parc Valrose, F-06108 Nice, France

<sup>g</sup> Office National d'Etudes et de Recherches Aérospatiales, B.P. 72, F-92322 Chatillon, France

<sup>h</sup> European Southern Observatory, Karl-Schwarzschild-Strasse 2, D-85748 Garching, Germany

<sup>i</sup> ASTRON, P.O. Box 2, NL-7990 AA Dwingeloo, The Netherlands

<sup>j</sup> Institute of Astronomy, ETH Zurich, CH-8092 Zurich, Switzerland

<sup>k</sup> Universit at van Amsterdam, Kruislaan 403, NL-1098 SJ Amsterdam, The Netherlands

## ABSTRACT

SPHERE, the ESO extra-solar planet imager for the VLT is aimed at the direct detection and spectral characterization of extra-solar planets. Its whole design is optimized towards reaching the highest contrast in a limited field of view and at short distances from the central star. SPHERE has passed its Final Design Review (FDR) in December 2008 and it is in the manufacturing and integration phase. We review the most challenging specifications and expected performance of this instrument; then we present the latest stage of the design chosen to meet the specifications, the progress in the manufacturing as well as the integration and test strategy to insure gradual verification of performances at all levels.

**Keywords:** exo-solar planets, extreme adaptive optics, coronagraphy, dual band imaging, polarimetry, spectral imaging

## 1. INTRODUCTION

The top objective of the Spectro-Polarimetric High-contrast Exoplanet Research (SPHERE) instrument for the VLT is the discovery and study of new extra-solar giant planets orbiting nearby stars by direct imaging of their circumstellar environment. The design of SPHERE is optimized towards reaching the highest contrast in a limited field of view and at short distances from the central star. Both evolved and young planetary systems will be detected, respectively through their reflected light (mostly by visible differential polarimetry) and through the intrinsic planet emission (using IR differential imaging and integral field spectroscopy). The design of SPHERE and its expected performance has been the subject of prior publications [1], [2] and [3].

The primary goal of extra-solar planet science of the next decade will be a better understanding of the mechanisms of formation and evolution of planetary systems. The fundamental observational parameter is the frequency of planets as a function of mass and separation. Theoretical models of planet formation predict that the peak of formation of giant

---

<sup>1</sup> francois.wildi@unige.ch

planets is found close to the snowline, thanks to the availability of a larger amount of condensate in the proto-planetary disk. In outer regions, the longer timescales involved should make planet formation a less efficient process. Migration mechanisms and long term orbit instabilities will alter the original distribution. Determination of the frequency of giant planets in wide orbits (> 5-10 AU) will allow testing basic aspects of the planet formation models.

While radial velocity spectroscopy remains the best technique currently available to study the inner side of the planet distribution with semi-major axis (<5 AU), high-resolution, high contrast imaging like that provided by SPHERE or GPI (ref) is expected to be the most efficient technique to discover planets in the outer regions of planetary systems. Current results from direct imaging surveys allow excluding only planet distributions with a large population of massive planets in outer orbits. With its enhanced capabilities (a gain of two orders of magnitudes in contrast with respect to existing instruments) and a list of potential targets including several hundred stars, SPHERE will provide a clear view of the frequency of giant planets in wide orbits. With the number of expected detections (several tens), the level of the large separation wing of the distribution with semi-major axis can probably be estimated with an accuracy of about 20-30%, good enough for a first statistical discussion of the properties of planetary systems. Beside frequency, it would also be interesting to derive the distributions of planets parameters such as mass, semi-major axis and eccentricities.

Furthermore, a direct imager like SPHERE provides the only way of obtaining spectral characteristics for outer planets. The SPHERE differential polarimetric channel (ZIMPOL) might also allow detecting a few planets shining by reflecting stellar light. Such an instrument will provide invaluable information with which to hone models in preparation for the ELTs and Darwin era. SPHERE will be highly complementary to current and contemporaneous studies of exo-planets.

## 2. SYSTEM DESIGN

By definition, the design of SPHERE was essentially frozen at the FDR, however, because SPHERE is rated as a fast track project by ESO, it was understood that the detailed design of certain components was not complete as long as it was demonstrated that the critical aspects had been dealt with. One aspect worth mentioning has been addressed since FDR: the control of scattered light.

We have obtained hemispheric reflectance measurements of different samples of black surface treatments, including standard organic black anodize, inorganic or mineral black anodize as per ESA standard ECSS-Q70-03, and space qualified black paint, PU1 and PNC (MAP). A sample of black gelcoat, foreseen for the interior surface of the CPI cover, was also measured.

The organic black coloring of anodized surfaces indeed have very poor performance in the NIR, taking off from the 5% level at ~700nm, reaching the 50% level at around 1 $\mu$ m. On the other hand the two painted samples, the black gelcoat, and the inorganically colored black anodize all have a flat reflectance spectrum, within the range of 3-6%, see figure 1. Therefore, for SPHERE, organic black coloring of anodized surfaces should be avoided. This is critical for the infrared paths (950 to 2320nm), but also valid for the visible paths, since the reflectivity of this treatment at 900nm is of the order of 30%. Inorganic coloring of anodized surfaces, the black gelcoat and the two paints, are acceptable across both wavelength ranges, well within our spec of 10%. The PNC paint (#2) has the lowest reflectivity and should therefore be preferred for baffles and light traps.

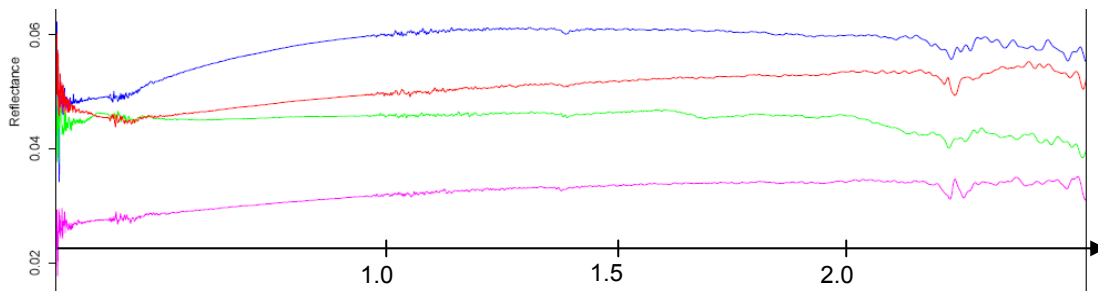


Fig. 1: Integrated  $2\pi$  reflectance of black surface treatments. PNC pain in pink, PU1 pain in red, black gelcoat in green, anorganic anodize in blue. X-axis ticks in micron, Y-axis ticks 2%, 4% and 6%

### 3. COMMON PATH HARDWARE

SPHERE is divided into four subsystems: the Common Path and Infrastructure (CPI) and the three science channels, a differential imaging camera (IRDIS, InfraRed Dual Imaging Spectrograph), an Integral Field Spectrograph (IFS) and a visible imaging polarimeter (ZIMPOL, Zurich Imaging Polarimeter). The Common Path includes pupil stabilizing fore optics (tip-tilt and rotation), calibration units, the SAXO extreme adaptive optics system, and NIR and visible coronagraphic devices. ZIMPOL shares the visible channel with the wavefront sensor through a beamsplitter, which can be a grey (80% to ZIMPOL) beamsplitter, a dichroic beamsplitter, or a mirror (no ZIMPOL observations). IRDIS is the main science channel and does imaging over a square field of 11 arcsec in one or two simultaneous spectral bands or two orthogonal polarizations and low and medium resolution long slit spectroscopy. The IFS, working from 0.95 to 1.65  $\mu\text{m}$ , provides low spectral resolution ( $R \sim 30$ ) over a limited,  $1.8'' \times 1.8''$ , field-of-view. A photon sharing scheme has been agreed between IRDIS and IFS, allowing IFS to exploit the NIR range up to the J band, leaving the band deemed optimal for the DBI mode to IRDIS for the main observation mode. This multiplexing optimizes the observational efficiency. In the opto-mechanical lay-out of SPHERE is shown at the left of Fig. 2 and the current implementation of SPHERE at the Nasmyth focus of the VLT is shown at the right of Fig. 2.

#### 3.1 Common Path and Infrastructure (CPI)

The common path is a large bench mounted on a triplet of active dampers, to which each science instrument will dock as a whole. When in operation on the Nasmyth platform A of the VLT UT3, SPHERE will be entirely enclosed in a thermal/dust cover and include a comprehensive automated cryo-vacuum system supplying 4 cryostats and a separate vacuum container.

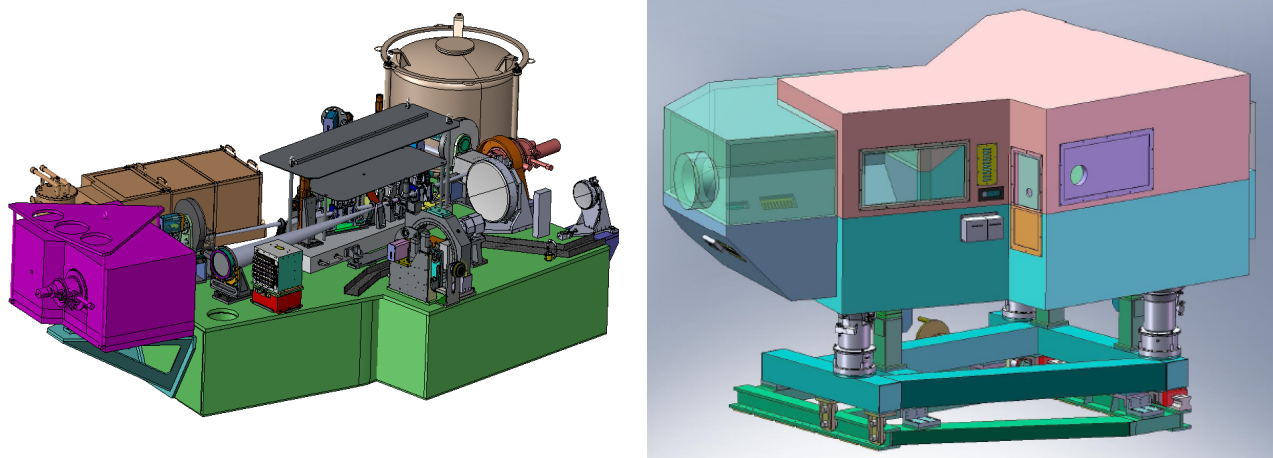


Fig. 2: The view on the left shows the complete SPHERE opto-mechanical assembly. The view on the right shows how SPHERE will look like in operation, when the opto-mechanical assembly is mounted onto the vibration damping system and into the thermal-vacuum enclosure. To facilitate integration and operations, this enclosure has separate modules for the IFS and ZIMPOL mount, so that this instrument can be mounted and dismounted with limited impact.

Besides classical optical components, the common path embeds various innovative components which have been the subject to a specific R&D effort in the project: toroidal mirrors manufactured by spherical polishing of pre-stressed substrates [4], achromatic 4 quadrants coronagraph [5], and apodized Lyot coronagraphs [6], variable spatial filter [8].

SPHERE uses 3 toroidal mirrors of 27, 133 and 366mm clear aperture. The largest and the smallest are polished already. Both are within the specification for high frequency errors. The largest is slightly above specifications in low spatial frequencies which will require compensation with the DM.

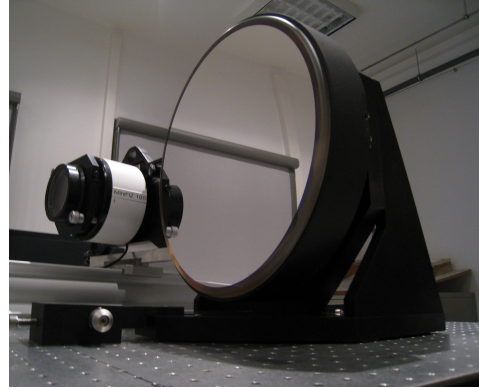
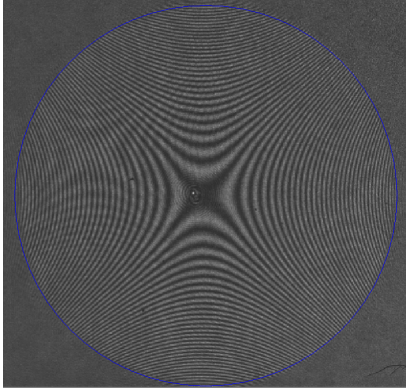


Fig. 3: Views of the toric mirror #3: The interferogram and the mirror integrated in its cell. The clear aperture is 366mm



Fig. 4: The manufacturing of opto-mechanical components is progressing fast. The variable spatial filter (L/h) and one of the coronagraph focal plane wheel (R/h) are shown here.

### 3.2 Extreme adaptive optics (SAXO)

SAXO is made of 3 real time loops and a sophisticated off-line calibration of non common path aberrations [7,14]. The main AO loop runs at 1200Hz and corrects for atmospheric, telescope, common and non common path defects, the 2<sup>nd</sup> loop runs at 0.1Hz and corrects the beam wander by tracking and correcting pupil shifts in real time. The last loop runs at around 10Hz and deals with the differential tip and tilt between the visible and infrared path; it guarantees that the target star is constantly centered on the infrared coronagraph. This AO system was very demanding in terms of R&D and numerous components have been developed specifically for it: a high order deformable mirror from CILAS, a dedicated electron multiplying CCD and camera for wavefront sensing, and a variable spatial filter for WFS aliasing reduction.

The 41x41 actuator High Order DM of 180 mm diameter is now delivered and displays a best flat of 5nm rms surface and maximum mechanical stroke  $> \pm 3.5 \mu\text{m}$  (Fig. 5). The high bandwidth tip-tilt mirror with a 0.5 mas rms on sky resolution was developed by the LESIA.

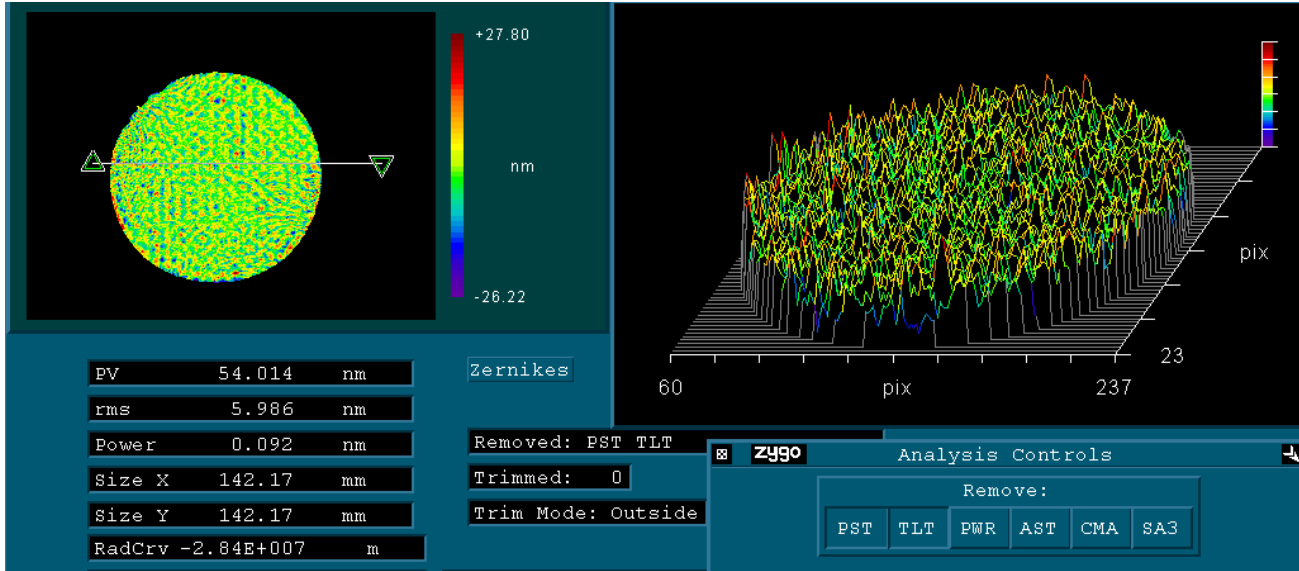


Fig. 5: Measurement of the surface quality of the high order deformable mirror. The original measurement is filtered to remove all the special frequencies that can be removed by the deformable itself ( $f > 1/9\text{mm}$ ).

The wavefront sensor is a 40x40 lenslet Shack-Hartmann, covering the 0.45-0.95  $\mu\text{m}$  spectral range, and equipped with a focal plane spatial filter [3], [8] continuously variable in size from  $\lambda/d$  to  $3\lambda/d$  at 0.7  $\mu\text{m}$ , where  $d$  is the sub-aperture diameter, for aliasing control. It is based on the dedicated 240x240 pixel electron multiplying CCD220 from EEV and achieves a temporal sampling frequency  $> 1.3 \text{ kHz}$  with a read-out noise smaller than  $1 e^-$

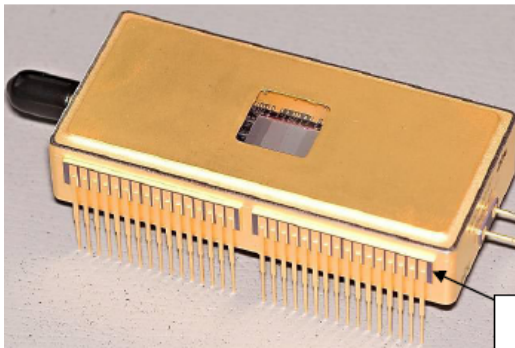
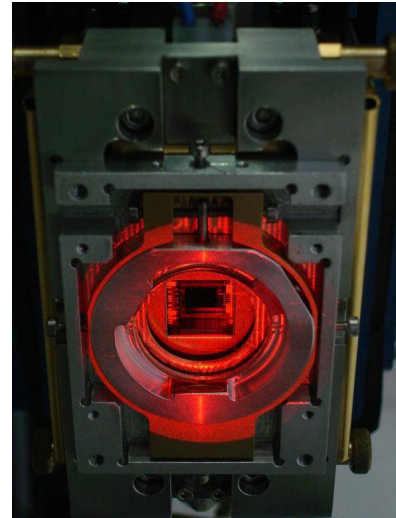


Fig. 6: The 256x256 EMCCD from E2V has now been delivered sample quantities. It is packaged in a Peltier cooled metallic case (L/h). The prototype camera equipped with a 40x40 lenslet array and read-out electronics is now operating. It produced Shack-Hartmann spots at 1360 frames per second with sub-electron noise. (R/h)

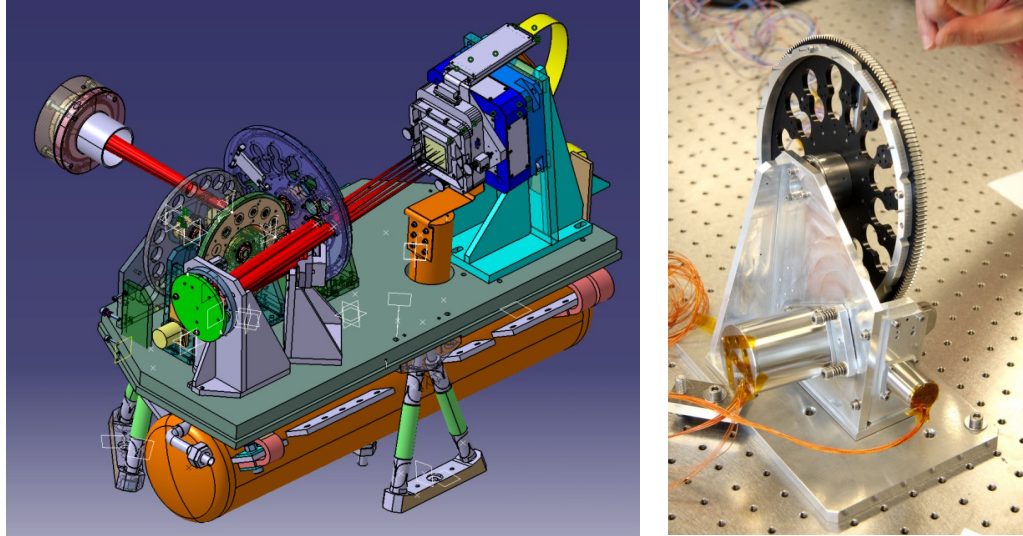


Non-Common Path Aberrations will be measured with phase diversity. During a first measurement step, the wavefront aberrations from the SPHERE input focus to the DBI camera will be measured using a point source at the input focus. In a second step the wavefront aberrations from the coronagraphic focus to the DBI camera will be measured, using a double source in the coronagraphic focus. By subtraction of these aberrations from the first ones, it shall be possible to determine and pre-correct the aberrations between input focus and coronagraphic mask so that the PSF is very consistent in time which leads to a reduction of persistent speckles.

## 4. IRDIS, THE DUAL BAND IMAGER AND SPECTROGRAPH

IRDIS design and performance predictions have been the subject to several communications already (p. ex. [9], [10]). When SPHERE is operating in survey mode, IRDIS operates in dual band imaging (DBI) but it also has dual polarimetry and slit spectroscopy capability; using its dual filter wheel for simultaneous polarization measurements and its Lyot wheel to hold the dispersive elements for spectroscopy.

Fig 7: The L/h picture is a 3D view of the IRDIS opto-mechanics (w/o the cryostat). The dual beams produce their image on the same detector, located on a dithering stage on the right side of the bench. The R/h pictures shows the cryo dual filter wheel which has already been successfully qualified in precision and repeatability.



The figure 8 below, shows the contrast versus angular separation that is expected with IRDIS in DBI.

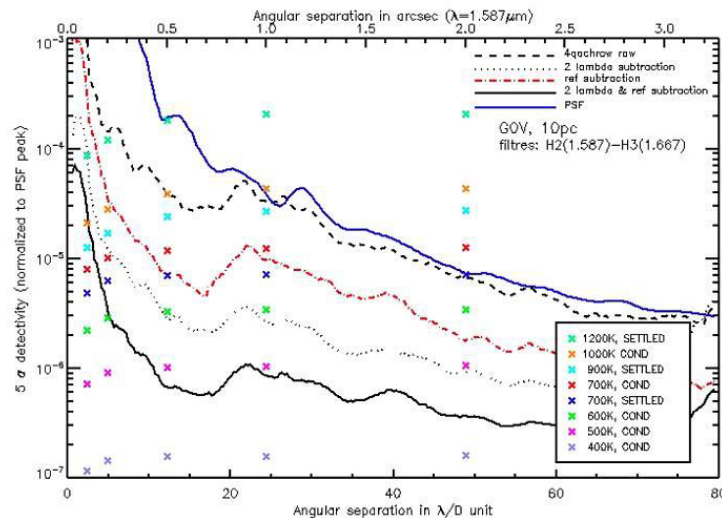


Fig 8: Some results of an extensive simulation of test cases involving various stellar ages and distances. Companion intensities (crosses) are compared with radial variance profiles in the processed images, assuming a G0V star at 10pc observed in the H2-H3 filter couple. COND refers to models for a condensed atmospheres free of dust, while SETTLED refers to atmosphere with rainout of refractory material (from [9])

## 5. THE INTERGAL FIELD SPECTROGRAPH

To explore the innermost part of the field, SPHERE has a spectro-imager called IFS. This instrument has a field of 145x145 pixels covering a field of 1.8" x 1.8" and can resolve the image spectrally with a resolution of 50 in the 0.95-1.35 $\mu$ m band or with a resolution of 30 in the 0.95-1.7  $\mu$ m band [11], [12].

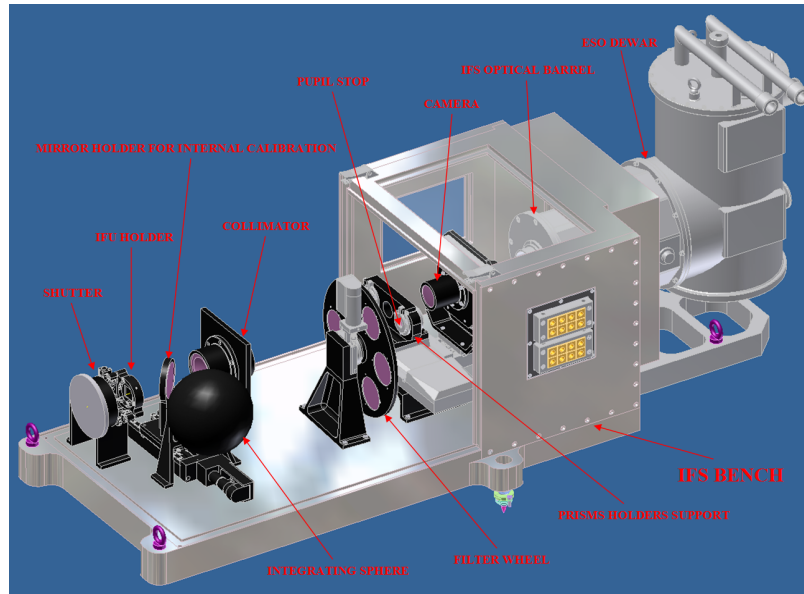


Fig 9: From the opto-mechanical point of view IFS is a relatively simple instrument: The IFS performs the spatial sampling of the field and the demagnification of the pixels. The light from each pixel is collimated, before going through the disperser. The disperser disperses the light from each pixel into a spectrum, which is imaged on the detector by the camera. Only the detector and the last lens are nitrogen cooled.

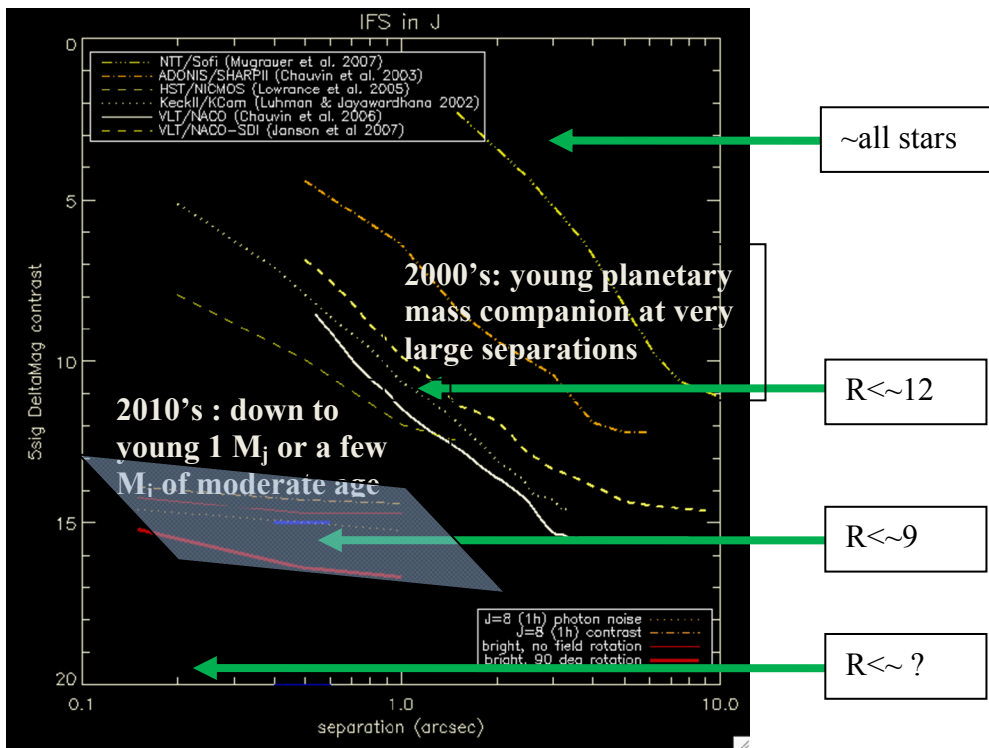
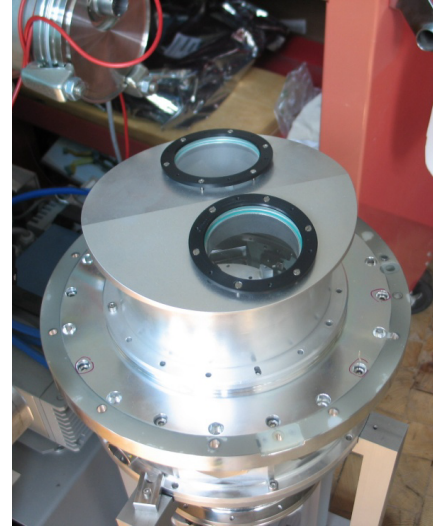
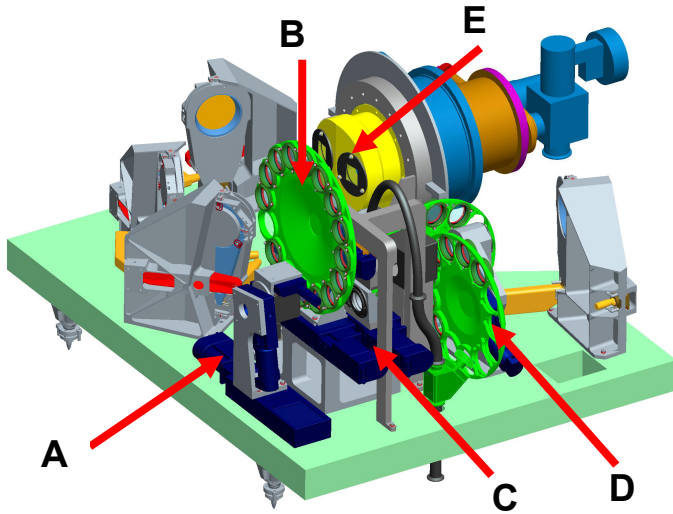


Fig 10: Contrast versus angular separation in the case of the IFS. This plot compares the IFS performance (red curve at the bottom left) to the capability of current instruments. The first detections are restricted to very favorable cases, in young system at large separation and massive giant planets. We enter with SPHERE in the real domain where numerous giant planet are expected, moderate separations and 1 to few Jupiter masses.

## 6. ZIMPOL, THE ZURICH POLARIMETER

ZIMPOL (Zurich Imaging Polarimeter) is located behind SPHERE's visible coronagraph. Among its main specifications are a bandwidth of 500 to 900 nm and an instantaneous field of view of  $3 \times 3$  arcsec<sup>2</sup> with access to a total field of view of 8 arcsec diameter by an internal field selector. The ZIMPOL optical train contains a common optical path that is split with the aid of a polarizing beamsplitter in two optical arms. Each arm has its own detector, but they are both located in the same cryostat and cooled to  $-80^{\circ}\text{C}$ . Above the beam splitter, the path contains common components for both arms like calibration components, common filters, a rotatable half wave plate and a ferroelectric liquid crystal polarization modulator. The two arms have the ability to measure simultaneously the two complementary polarization states in the same or in distinct filters. The images on both ZIMPOL detectors are Nyquist sampled at 600 nm.

The principle of ZIMPOL and its performance have been addressed in [13].



Figures 11: L/h: 3D view of ZIMPOL Opto-mechanics. A) polarization equalizer (1<sup>st</sup> optical component in the path), B) Calibration components wheel, C) ferroelectric liquid crystal (FLC) modulator which is the center piece of the ZIMPOL system, D) 2 other wheels allow different bands to be measured simultaneously in the 2 arms, E) Cryostat holding the 2 detectors for the 2 arms. R/h the engineering detectors are already been integrated in the cryostat.

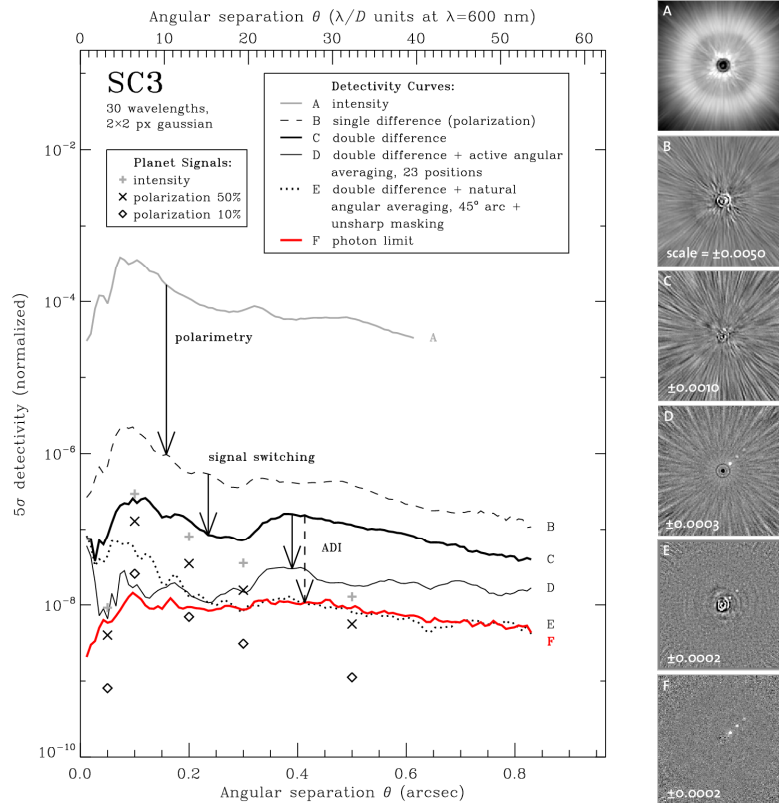


Fig 12: **L/h:** The 5sigma detectivity, plotted as a function of angular separation at various stages of the noise reduction process, including three differential methods. The symbols denote the typical level of planet reflected light around a very nearby star. **R/h:** The two-dimensional images at each stage, assuming 50% polarized planets. Note: the use of 4-quadrant coronagraph in good conditions may improve the detectivity at the closest separations ( $< 0.3$  arcsec).

## 7. INTEGRATION OPERATIONS

With 3 science channels, complete with opto-mechanics, optics, detector, instrument software data deduction software, a complex multi-loop AO system and 11 institute formally involved, the integration and test of SPHERE is a complex and potentially risky process. This is why a multi-level approach is taken, much in the spirit of space programs:

The technical specification applicable to SPHERE has been revisited to derive specifications applicable to each of the four sub-systems (Common Path and the 3 science channels). Each sub-system is goes through an Assembly, Integration and Test phase during which every aspect is brought into play including instrument software and reduction recipes. After this phase a formal acceptance takes place and the sub-system is transferred to the final system integration location.

At the system integration location, even though significant real estate is provisioned, much care is take to sequence the operations in an optimal way:

- Mechanical and optical interfaces between science channels and Common Path are checked in advance with dummies
- Space and time is provided for the reassembly of science channels after transfer and a functional check-out is performed before integration with the Common Path.
- To minimize personnel interference, science channels are integrated with the Common Path and characterized one at a time before the complete system tests are performed

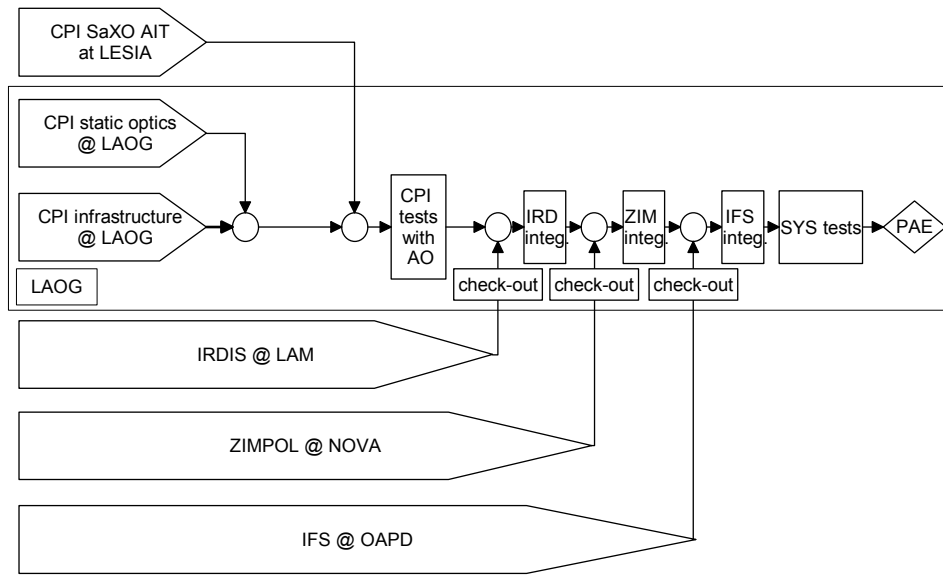


Fig 13: Flow chart of the AIT operations. In the large rectangle, the operations performed at the main integration site in Genoble are listed. The three science channels are represented below. Above the main rectangle, the integration of the AO system is represented. Given its complexity, it is integrated in a separate location, while the static optics of the Common Path undergo AIT in Grenoble.

## 8. CONCLUSION

We have presented here the status of the SPHERE instrument during the manufacturing stage. The Final Design Review was successfully passed in Dec. 2008 and we expected to start integration of the four sub-systems in the fall of 2009. A lot of functional units have already been manufactured, some keystone elements are performance tested and accepted already. The instrument software is expected to be ready at the end of 2009 and we are getting ready for a very busy 2010 where all sub-system will reach their acceptance and the major part of system integration and test will take place. Transfer to Paranal Observatory is scheduled for the 1<sup>st</sup> half of 2011 and the beginning of operation by about mid 2011.

## REFERENCES

- [1] Jean-Luc Beuzit, Markus Feldt, Kjetil Dohlen, David Mouillet, Pascal Puget, Francois Wildi, Lyu Abe, Jacopo Antichi, Andrea Baruffolo, Pierre Baudoz, Anthony Boccaletti, Marcel Carbillet, Julien Charton, Riccardo Claudi, Mark Downing, Christophe Fabron, Philippe Feautrier, Enrico Fedrigo, Thierry Fusco, Jean-Luc Gach, Raffaele Gratton, Thomas Henning, Norbert Hubin, Franco Joos, Markus Kasper, Maud Langlois, Rainer Lenzen, Claire Moutou, Alexey Pavlov, Cyril Petit, Johan Pragt, Patrick Rabou, Florence Rigal, Ronald Roelfsema, Gérard Rousset, Michel Saisse, Hans-Martin Schmid, Eric Stadler, Christian Thalmann, Massimo Turatto, Stéphane Udry, Farrokh Vakili, Rens Waters, "SPHERE: a 'Planet Finder' instrument for the VLT", *Ground-based and Airborne Instrumentation for Astronomy II*, SPIE 7014-42 (2008)
- [2] F. Wildi, J.-L. Beuzit, M. Feldt, D. Mouillet, K. Dohlen, P. Puget, A. Baruffolo, J. Charton, J. Antichi, P. Baudoz, A. Boccaletti, M. Carbillet, R. Claudi, Ph. Feautrier, E. Fedrigo, T. Fusco, R. Gratton, N. Hubin, M. Kasper, M. Langlois, R. Lenzen, C. Moutou, A. Pavlov, C. Petit, J. Pragt, P. Rabou, R. Roelfsema, M. Saisse, H.-M. Schmid, E. Stadler, Ch. Thalmann, M. Turatto, S. Udry, R. Waters, T. Henning, A.-M. Lagrange, F. Vakili., "The SPHERE exoplanet imager: Status report at PDR", *Astronomical Adaptive Optics Systems and Applications III*, SPIE 6691-18 (2007)
- [3] K. Dohlen, JL Beuzit, M. Feldt, D. Mouillet, P. Puget, F. Wildi, J. Charton, C. Moutou, A. Longmore, T. Fusco, A. Boccaletti, P. Baudoz, P. Rabou, Ph. Feautrier, M. Langlois, M. Saisse, R. Gratton, J. Antichi, A. Berton, HM.

- Schmid, R. Waters, "SPHERE, a planet finder instrument for the VLT." in *Ground-based and Airborne Instrumentation for Astronomy*. SPIE 6269 (2006)
- [4] E. Hugot, M. Ferrari, K. El-Hadi, G. R. Lemaître, P. Montiel, "Stress polishing of toric mirrors for the SPHERE common path", in *Advanced Optical and Mechanical Technologies*, SPIE 7018-5 (2008)
- [5] Anthony Boccaletti "Prototyping achromatic coronagraphs for exoplanet characterization with SPHERE", in *Adaptive Optics Systems*, SPIE 7015-46 (2008)
- [6] G. Guerri, S. Robbe-Dubois, J.-B. Daban, L. Abe, R. Douet, Ph. Bendjoya, F. Vakili, M. Carbillet, "Apodized Lyot coronagraph for the VLT instrument SPHERE: laboratory tests and performances of a first prototype in the visible", in *Ground-based and Airborne Instrumentation for Astronomy II*, SPIE 7014-124 (2008)
- [7] C. Petit, T. Fusco, J.-M. Conan, J.-F. Sauvage, G. Rousset., P. Gigan, J. Charton, D. Mouillet, P. Rabou, M. Kasper, E. Fedrigo, N. Hubin, Ph. Feautrier, J.-L. Beuzit, P. Puget, "The SPHERE XAO system: design and performance", in *Adaptive Optics Systems*, SPIE 7015-65 (2008)
- [8] T. Fusco, C. Petit, P. Rabou, K. Dohlen, D. Mouillet, Pascal Puget, "Optimization of a spatially filtered Shack-Hartmann wavefront sensor", in *Adaptive optics systems*, SPIE 7015-54 (2008)
- [9] K. Dohlen, M. Langlois, M. Saisse, L. Hill, A. Origine, M. Jacquet, Ch. Fabron, J.-C. Blanc, M. Llored, M. Carle, C. Moutou, A. Vigan, A. Boccaletti, M. Carbillet, D. Mouillet, J.-L. Beuzit "The infrared dual imaging and spectrograph for SPHERE: design and performance", in *Ground-based and Airborne Instrumentation for Astronomy II*, SPIE 7014-126 (2008)
- [10] A. Vigan and M. Langlois and C. Moutou and K. Dohlen, "Long slit spectroscopy for exoplanet characterization in SPHERE", *Ground-based and Airborne Instrumentation for Astronomy II*, SPIE, 7014-
- [11] R. Claudi, M. Turatto, R. Gratton, J. Antichi,; E. Cascone,; V. De Caprio,; S. Desidera, D. Mesa, S. Scuderi, "SPHERE IFS: the spectro differential imager of the VLT for exoplanets search", in *Ground-based and Airborne Instrumentation for Astronomy II*, SPIE 7014-119 (2008)
- [12] S. Desidera, R. Gratton, R. Claudi, J. Antichi, D. Mesa, M. Turatto,; P. Bruno, E. Cascone,; V. De Caprio, E. Giro; S. Scuderi; M. Feldt, A. Pavlov, K. Dohlen, J-L Beuzit, D. Mouillet, P. Puget, F. Wildi, "Calibration and data reduction for planet detection with SPHERE-IFS", in *Ground-based and Airborne Instrumentation for Astronomy II*, SPIE 7014-127 (2008)
- [13] Ch. Thalmann, H.-M. Schmid, A. Boccaletti, D. Mouillet, K. Dohlen, R. Roelfsema, M. Carbillet, D. Gisler, J.-L. Beuzit, M. Feldt, R. Gratton, F. Joos, Ch. U. Keller, J. Kragt, J. H. Pragt, P. Puget, F. Rigal, F. Snik, R. Waters, F. Wildi, "SPHERE ZIMPOL: Overview and performance simulation", in *Ground-based and Airborne Instrumentation for Astronomy II*, SPIE 7014-120 (2008)
- [14] J.-F. Sauvage, T. Fusco, G. Rousset, C. Petit, "Calibration and pre compensation of non commo path aberrations for extreme adaptive optics", in *JOSAA*, 24, 8, pp. 2334-2346, (2007)